Available online at www.sciencedirect.com

ScienceDirect

Procedia Engineering 126 (2015) 73 – 77

Procedia Engineering

www.elsevier.com/locate/procedia

7th International Conference on Fluid Mechanics, ICFM7

Investigations on the feature of turbulent viscosity associated with vortex shedding

Q. Li, Q. W. Ma*, S.Yan

School of Mathematics, Computer Science and Engineering, City University London Northampton square, London, EC1V 0HB, UK

Abstract

The main purpose of this paper is to investigate the turbulent viscosity, particular its spatial distribution, in the flow around a fixed or moving cylinder. For this purpose, two-dimensional numerical simulations of turbulent flow is performed using the OpenFOAM, in which the Reynolds-averaged Navier-Stokes (RANS) equation, with either k-ε or k-ω SST turbulent model, is solved using the finite volume method. The numerical model is validated by using both experimental and numerical results in terms of the mean drag coefficients and the Strouhal number. Turbulent viscosity is significant only in a confined area around the vortex shedding (critical area), and the width of the critical area is considerably affected by the Reynolds numbers (Re) and the motion of the cylinder.

Peer-review under responsibility of The Chinese Society of Theoretical and Applied Mechanics (CSTAM)

Keywords: Turbulent Viscosity; Vortex Shedding; Turbulent Model; Numerical Modelling

1. Introduction

In the offshore and marine engineering, cylindrical structures, such as the legs of Jack up platforms and the foundations of offshore wind turbines, are commonly used. These structures are exposed to tidal current and water waves. Due to their relatively low Keulegan Carpenter number, the viscous/turbulent effects, e.g. the vortex induced vibration/motion, may be significant. The typical range of the Reynolds numbers (Re) associated with this problem is 40 to 10^6, corresponding to a pile with diameter of 0.5m subjected to tidal flow up to 2m/s [1]. In order to numerically simulate such problem, the Reynolds-Averaged Navier-Stokes (RANS) equation with appropriate

* Corresponding author. Tel.: +0044-20-7040-8159; fax: +0044-20-7040-8566.
E-mail address: Q.Ma@city.ac.uk

Peer-review under responsibility of The Chinese Society of Theoretical and Applied Mechanics (CSTAM)
doi:10.1016/j.proeng.2015.11.181

turbulent model for evaluating the turbulent viscosity is often used. However, it has been revealed by many researchers (e.g. [1]) that different turbulent models give significant different prediction of the hydrodynamic parameters, e.g. the drag/lift forces and vortex shedding frequencies, due to the difference in modelling the turbulent viscosity. A further exploration of the feature of the turbulent viscosity benefits the selection of an appropriate turbulent model to ensure the reliability of the numerical prediction. On the other hand, it is generally agreed that solving the RANS with turbulent model (referred to as NS model) is a time-consuming task, and a state-of-the-art strategy to accelerate the numerical modelling is to combine the NS model with other more computationally efficient models with certain degrees of simplification (referred to simplified model), e.g. the potential theory, which assumes the flow is inviscid and irrotational, or laminar NS solver ignoring the turbulence. The numerical approach adopting such strategy is usually referred to as a hybrid model. The theoretical hypothesis of the hybrid model is that the viscous/turbulent effects are only significant in limited area, e.g. near the offshore structures and breaking waves, and may be ignored in other areas. Two typical approaches have been attempted to realize this strategy. The first one is the spatially hierarchical approach (domain decomposition, e.g. [2]), in which the computational domain is decomposed into several subdomains: in the subdomain with significant viscous effects, the NS model is adopted; in other subdomains, simplified models are implemented. The second one is the model/velocity decomposition (e.g. [3-5]), in which a simplified model covers the entire computational domain and a complementary NS model is solved in a subdomain with significant viscous effects to correct the solution of the simplified models so that within this subdomain, the flow is governed by the NS model by summing the solution of the simplified model and that of the complementary NS model. This strategy improves the computational efficiency by limiting the computational domain governed by the time-consuming NS model to considerably small area. However, in both the domain-decomposition and the model-decomposition approaches, the size of the subdomain with significant viscous/turbulent effects is critical to obtain reliable results and is generally determined by comparing the results using different sizes with the experimental data for specific problems. One may agree that the size of the subdomain shall be closely related to the spatial variation of the turbulent viscosity or the vorticity. Nevertheless, systematic investigation considering features of spatial variation of turbulent viscosity is rarely found in the public domain.

In this study, the feature of the turbulent viscosity near a circular cylinder subjected to uniform current is numerically investigated using the open source software, OpenFOAM. Only two-dimensional cases are presented in this paper. The cylinder is either fixed or subjected to a forced periodic vibration. For the former, the parameters of drag coefficient and Strouhal number obtained in this work are compared with experimental data and numerical results from other publications. We aim to shed lights on two specific questions: (1) which turbulent model can well predict the turbulent viscosity near the structure? And (2) how the significance of the turbulent viscosity spatially varies? The answers to these questions may benefit selections of appropriate turbulent models or development of hybrid models for fluid-structure interaction in offshore and marine engineering.

2. Numerical model

The open-source solver OpenFOAM is based on the finite volume method (FVM) to solve incompressible transient fluid-structure interaction. In this model, the PISO/PIMPLE loop is adopted, where continuity, momentum equations are solved simultaneously using Rhie–Chow pressure interpolation. The Reynolds-averaged Navier-Stokes equation (RANS) incorporating a turbulent model is applied to simulate the turbulent flow. A rectangular computational domain is used in the numerical simulation. The length and the width of the computational domain are $60D$ and $40D$ respectively, where D is the diameter of the cylinder. A circular cylinder is located in the central longitudinal axis with its centre being $20D$ away from the upstream boundary of the computational domain. A detailed configuration can be found in [1]. The boundary conditions applied at the left end (upstream) and right end (downstream) are the velocity inlet and the pressure outlet, respectively. On the top and bottom boundaries, the free slip condition is applied. The computational mesh is generated by using the OpenFOAM internal functions. Different mesh sizes will be used in the numerical investigations based on the convergent tests. Both k-ε and k-ω SST turbulent models are used in the investigations. In the study, the Re is defined as $\mathrm{Re} = UD/\gamma$ where U and γ are the freestream/inlet velocity and the physical kinematic viscosity of the water, respectively. The drag force F_D is expressed as the drag coefficient, C_D, using $C_D = 2F_D / \rho U^2 D$ where ρ is the density of the water.

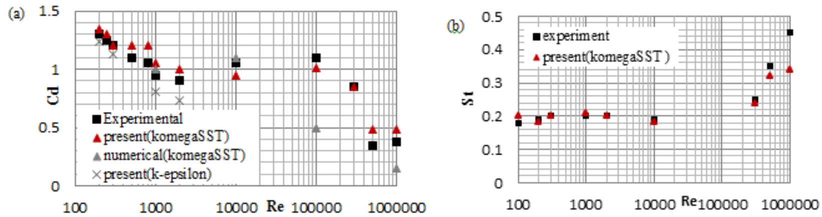

Fig.1 Comparison of (a) mean drag coefficient and (b) Strouhal number in cases with different Re (Experimental data are duplicated from [8] and [9] , R.M. Stringe's results are duplicated from [1])

3. Numerical results and discussions

3.1 Validation

The numerical model is validated by using the cases with a fixed cylinder. The experimental results of the drag coefficients by Wieselsberger [6] for 40<Re< 5×10^5 and Schewe [7] for Re > 10^5 and corresponding numerical results by Stringer *et al* [1] are used for comparison. It is well understood that for low Re (e.g. 40), the flow is laminar and can be numerically simulated using a steady model. The vorticity in such case is symmetrical about the central longitudinal axis of the cylinder as demonstrated by [1]. When Re >40, the wake becomes unstable, which eventually leads to a vortex shedding alternately occurring at either side of the cylinder at a certain frequency, resulting in the oscillation of the drag coefficient. In such case, the mean drag coefficient Cd and the Strouhal number ($S_t = fD/U$) which normalizes the vortex-shedding frequency (*f*), are critical and of most importance. The comparisons of Cd and St are displayed in Fig.1. From Fig. 1 (a), it is found that Cd predicted by the present method with k-ω SST turbulent model generally agrees well with the experimental data. The maximum relative difference is around 13% at Re $>5\times10^5$ due to the limitation of the RANS in capturing small-scale eddies. It should be pointed out that Stringer *et al* [1] used the OpenFOAM with k-ω SST turbulent model to predict Cd for Re within the same range but gave significantly different results as shown in Fig.2 (a), especially at Re = 10^5 where vortex shedding is not observed in Stringe *et al* [1] but is found in the present study with k-ω SST turbulent model. One may also observe from Fig.1(b) that the Strouhal number predicted using the present method with k-ω SST turbulent model agree well with the experimental data in a large range of Re except the case with Re=10^6. This implies that the present method with k-ω SST turbulent model can produce reliable results for analyzing the feature of the turbulent viscosity and vorticity.

From Fig.1 (a), one may also notice that the present method with k-ε model seems to significantly underestimate Cd when Re ≤ 2000. The difference between the results with k-ε model and the experimental data, as well as the present results with k-ω SST model, become more significant when Re >2000. For clarity, the results are not shown in Fig.1 (a). As indicated in the Introduction, the success of the RANS on modelling the turbulent flow largely relying on the reliability of the turbulent model on estimating the turbulent viscosity. The k-ε model embedded in the OpenFOAM is theoretically a low-Re turbulent model, which gives fairly good prediction for the case with Re < 100. However, for relatively higher Re (e.g. 1000), the k-ε model seems to significantly underestimate the turbulent viscosity, especially at the areas covered by shed vortices (generally around 0.003 by k-ε model compared to approximately 0.005 by k-ω SST model), as demonstrated by Fig.2. It should be noted that the turbulent viscosities demonstrated in Fig.2 are those at the same time instant when the vortex is fully developed. For the same velocity field, the difference of the turbulent viscosity predicted by using the k-ε model and k-ω SST model may be insignificant. However, such small difference may be accumulated during the development of the vortex.

3.2 Feature of the turbulent viscosity

In order to explore the feature of the turbulent viscosity and its relation with the vorticity, corresponding results in the cases with different Re are presented in Fig.3. One may observe from this figure that (1) the pattern of the contour lines of the turbulent viscosity closely related to the spatial distribution of the vorticity. In the center of the vortex, the turbulent viscosity is relatively small; whereas in the area between two neighboring vortex, a relatively higher turbulent viscosity is observed; (2) for relatively high Re, i.e. Re = 1000 (Fig.2(b)) Re = 10^6 (Fig.3(b)), a significantly high turbulent viscosity is show in the gap between two newly generated vortex, which are not fully separated from the cylinder surface; however, such phenomenon is not found in the case with low Re, e.g. 200 (Fig.3(a)); (3) following the flow separation, the turbulent viscosity near the same vortex is weakened in a short duration after the vortex are shed away from the cylinder surface; it is then amplified when the shed vortex moves further downstream.

(a)

(b)

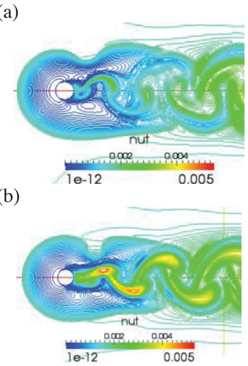

Fig.2. the distribution of the turbulent viscosity around the cylinder using (a) k-ε model and (b) k-ω SST (Re = 1000, fixed cylinder)

nut (turbulent viscosity) vorticity

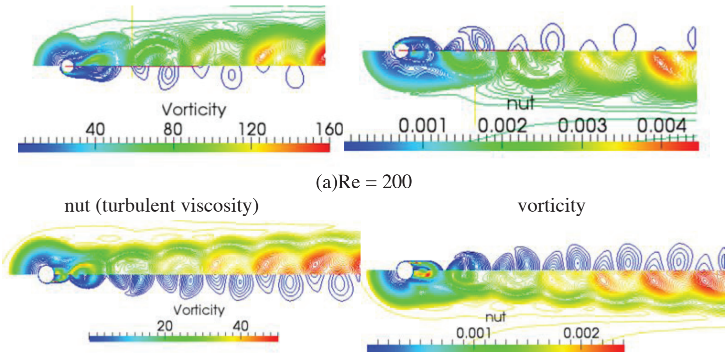

(a)Re = 200

nut (turbulent viscosity) vorticity

(b)Re = 1000000

Fig.3. Spatial distribution of vorticity and turbulent viscosity around the cylinder (left: y>0 (above the centre of the cylinder) right: y<0 (below the centre of the cylinder) k-ω SST, fixed cylinder)

(a) (b)

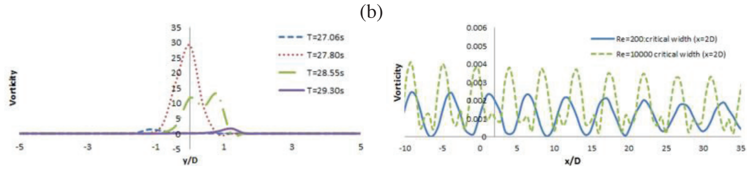

(a) Transversal distribution at x=2D with Re = 10000 (b) longitudinal distribution at $y = W_c/2$

Fig.4 Spatial distribution of vorticity in the cases with different Re (k-ω SST, fixed cylinder)

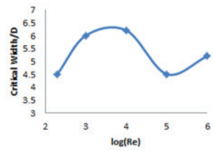

Fig.5. Critical width at x=2D (fixed cylinder)

One may also found from Fig. 3 that the turbulent viscosity and vorticity are significant in a confined area around the vortex shedding (critical area). The boundary of the critical area is defined by the contour line where the vorticity being 1% of the maximum vorticity on the cylinder surface. A similar definition was suggested by Edmund [5] for steady laminar flow, in which the critical area remains the same at different time step. However, for the cases with vortex shedding as presented here, the distribution of the vorticity varies at different time as demonstrated in Fig.4(a) which compares the distribution of the vorticity along a transversal axis through x = 2D, i.e. 2D downstream from the centre of the cylinder, within one shedding period with Re = 10000. As a result, the boundaries of the critical area at different time are different. In the case shown in Fig.4 (a), the widths of the critical area ranges from 2.8D to 6.2D. To reflect the unsteady behavior of the vortex shedding, the critical width, $W_{c,}$ in this study is defined as the maximum width of the critical area within one shedding period. Fig.5 displays W_c at x = 2D in the cases with different Re. It is interesting to find that the critical width shows an oscillating trend, i.e. increase as the increase of Re until Re =10^4, after which it reaches a trough at Re = 10^5 and increases again afterward. The critical width obviously varies along the longitudinal axis. In all cases studied in this paper, the critical width along the central longitudinal axis may reach 2W_c (x = 2D). This suggests that beyond the area confined by the longitudinal axis $y = \pm W_c$ (x = 2D) (corresponding to a critical area with width of 2W_c (x = 2D)), the vorticity and the turbulent viscosity is insignificant. This is demonstrated in Fig.4 (b), which shows that the magnitudes of the vorticity in the axis $y = \pm W_c$ (x = 2D) are insignificant (all below the threshold i.e. 1% of the maximum vorticity on the cylinder), although a clear periodic variation can be noticed. It shall be pointed out that the critical width discussed here only indicates the confined area where the vorticity and turbulent viscosity are significant. It does not mean that one can assign the width of the computational domain to be the critical width in order to achieve the same results as those presented here. Our numerical tests indicate that even the width of the domain is assigned to be $2W_c$ ($x = 2D$), the predicted drag coefficients may have difference with the results presented in Fig.1 at approximately 5%. For such domain size, even a potential solution is used to provide velocity and the pressure on the top and bottom walls of the computational domain (following the idea of domain-decomposition), no significant improvement in terms of drag coefficient prediction. A similar conclusion is made by Kim et al [4].

(a) (b)

Fig.6 vorticity distribution near moving cylinder at Re=185 for Fr=0.8 (a) and Fr=1.1 (b)

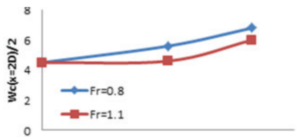

Fig.7. Critical width at x=2D in the cases with moving cylinders (Re = 185)

The effects of the motion of the cylinder on the vortex shedding and the critical width are also considered. To do so, the cylinder is subjected to a forced vibration along transversal direction with its displacement being $A\sin(2\pi f_c t)$, where A is the oscillating amplitude and f_c is the exciting frequency. The exciting frequency is specified by using the frequency ratio $F_r = f_c/f$, which ranges from 0.8 to 1.1 in this study. The oscillation amplitude ranges from $0.3D$ to $0.5D$. In this paper, only the results with Re = 185 is presented due to the limit of the space. It is observed that due to the effect of the exciting frequency, the shedding vortex does not follow the law of Strouhal and shows a non-regular pattern (as demonstrated in Fig.6), leading to considerable larger critical area than that in the corresponding case with fixed cylinder as shown in Fig.7. It is found that for specific exciting frequency, W_c increases as the increase of the oscillation amplitude; for specific oscillation amplitude, W_c is considerably affected by the exciting frequency.

4. Conclusions

This paper presents investigations of the feature of the turbulent viscosity associated with flow around both fixed and moving cylinder in the cases with different Re. The main conclusions include (1) the turbulent viscosity is significant only in a confined area around the vortex shedding (critical area); (2) The width of the critical area varies with the Reynolds number but the variation is between 8-14D in the cases investigated; (3) the motion of the cylinder may significantly affect the spatial distribution of the turbulent viscosity, enlarging the critical area. More discussions and details will be presented in the conference.

Acknowledgements

The first author is supported by the China Scholarship Council (CSC) project and City University London.

References

[1] R.M. Stringer, J. Zang, A.J. Hillis, Unsteady RANS computations of flow around a circular cylinder for a wide range of Reynolds numbers. Ocean Engineering. 87(2014), 1–9.

[2] M. Hafez, A. Shatalov, and E. Wahba, Numerical simulations of incompressible aerodynamic flows using viscous/ inviscid interaction procedures. Computer Methods in Applied Mechanics and Engineering 195 (2006), 3110- 3127.

[3] R. Luquet, P. Ferrant, B. Alessandrini, G. Ducrozet, and L. Gentaz, Simulation of a TLP in waves using the SWENSE scheme. In Proceedings of the Seventeenth International Offshore and Polar Engineering Conference, Lisbon, Portugal,2007, pp. 1916 -1922.

[4] K. Kim, A.I. Sirviente, R. F. Beck, The complementary RANS equations for the simulation of viscous flows, International Journal for Numerical Methods in Fluids, Vol. 48(2005)199-229.

[5] D. Edmund, A velocity decomposition method for efficient numerical computation of steady external flows. PhD thesis, University of Michigan, 2012.

[6] Wieselsberger, on the drag of circular cylinders, Physikalische Zeitschrift, vol. 22, 1992, pp. 219–224.

[7] G. Schewe, On the force fluctuations acting on a circular cylinder in cross flow from subcritical up to transcritical Reynolds Numbers. J. Fluid Mech. 133, 1983, pp. 265-285.